



TERMOTECNIA

Grupo de Investigación Reconocido de la Universidad de Valladolid
Unidad de Investigación Consolidada de Castilla y León UIC 053

<http://termotecnia.gir.uva.es/>

EXPERIMENTAL STUDY ON THE COOLING CAPACITY OF A RADIANT COOLED CEILING SYSTEM

*Manuel Andrés Chicote, Ana Tejero González, Eloy Velasco Gómez,
Francisco Javier Rey Martínez*

This is an **Accepted Manuscript** of an article published by **Elsevier**:

Energy and Buildings, 2012, Volume 54, Pages 207-214, ISSN 0378-7788

<https://doi.org/10.1016/j.enbuild.2012.07.043>





Abstract

Nowadays, radiant ceiling systems can be considered among the technologies capable of meeting sustainable heating and cooling requirements. In order to adequately address design and simulation issues concerning these systems, correct evaluation of the heat transfer process is needed.

The aim of this research is to present further evidence on the cooling capacity and heat transfer coefficients for a cooled radiant ceiling, assuring adequate thermal comfort levels in those possible different operation conditions. An experimental setup into a climate test room was developed and used to derive convenient results.

The obtained values revealed that heat transfer evaluations on the basis of operative temperature as the unique reference temperature and corresponding total coefficient are not appropriate in real situations, but considering radiant and convective phenomena separately is strongly recommended.

Keywords

Radiant ceiling cooling, heat transfer coefficients, sustainable cooling, passive cooling design, thermal comfort.



1 Introduction

Nowadays, buildings are responsible for up to 40 % of total energy consumption in the European Union. Moreover, the sector develops to improve social well-being by providing the best possible indoor environment, which is bound to increase energy use. However, at the same time, it has to adapt to the current economic, energetic and environmental crisis situation. In this context, improving energy efficiency and the use of renewable energy sources are important measures needed within the sector. [1]

In these terms, radiant ceiling systems are shown as an important alternative technology in order to meet current sustainable heating and cooling requirements. They belong to a group of systems which consist of large radiant surfaces arranged in room walls, floors or ceilings used for indoor climate conditioning in buildings. Their operation is based on heat transfer taking place between ceiling surface and its surroundings because of two different phenomena at the same time: room air convection and radiant long-wave exchange with other surfaces, which normally accounts for more than 50% of the total heat transfer [2]. In this respect, Miriel et al. [3] determined experimentally that the radiant component involves around 66 % of the total heat transfer in cooling operation and 80 % in heating operation. Predominance of the radiant heat transfer mechanism proved to be even greater in the experimental work conducted by Rahimi et al. [4] regarding a ceiling heating system.

These systems have been developed along the last decades and are now consolidated in Central and Northern Europe. However, they are not so widely spread in southern countries where climatic conditions are quite different [3].

They can be used for both heating and cooling. Nevertheless, cooled ceilings are the most interesting configuration due to the improvement of convective patterns and consequent greater total heat flows [5].

Radiant ceiling systems provide even better thermal comfort levels than conventional HVAC systems by means of appropriate surface temperature control and reduction of air movement. This permits to minimize draught discomfort and achieve more homogeneous temperature distribution into the occupied space [6].

Furthermore, involved large exchange areas allow temperature differences between the active surface and air to be reduced. Thus, in order to meet required thermal capacity, it is possible to use lower fluid temperatures for heating and higher fluid temperatures for cooling. This fact improves energy efficiency of the generation equipment and entails a reduction in energy consumption. In addition, this allows the use of alternative low-grade energy sources, such as geothermal energy, groundwater, favorable outdoor air (whose potential can be enhanced by evaporative cooling techniques [7, 8]) or recovered waste heat [9, 10, 11, 12].

Basically, cooled radiant ceilings could be arranged within two different energy concept designs:

- Low thermal inertia systems: These include technologies without energy storage periods, so asynchrony of cold generation and energy absorption in terminal units is not



provided. Common types are radiant suspended panels and embedded surface systems [10].

- o High thermal inertia systems: They are mainly represented by Thermally Activated Building Systems (TABS), which consist of pipes embedded in structural building elements serving as energy storage. Dynamic behavior is exploited to reduce peak loads and optimize cold generation [10, 11, 12, 13].

2 Objectives

Irrespective of the differences previously mentioned, heat transfer process between cooled ceiling surface and room is subject to the same physical phenomena for every type of system, providing a given cooling capacity as a function of its surface temperature and the temperature characteristics of the indoor environment. According to this and to the European standard EN 15377-1 [14], as a previous step to the system design and dimensioning process, it is therefore possible to establish a basic characteristic curve for cooling, which is independent of the type of system and applicable to all surfaces. Then, cooling output values obtained from this curve can be used to determine other design parameters of each particular system (for instance depth of the embedded pipe, pipe spacing, fluid supply temperature, etc.), so as to achieve the required surface temperature.

The standard EN 15377-1 establishes a unique correlation between the system cooling output and the difference between mean ceiling surface temperature and indoor operative temperature, as expressed in Eq. (1).

$$q_{\text{tot}} = 8.92 (T_{\text{op}} - T_s)^{1.1} \quad (1)$$

Similar general curves derive from other previous studies on ceiling cooling capacity estimation: Causone et al. [15] experimentally evaluated the radiant, convective and total heat transfer coefficients in typical conditions of occupancy of an office or residential building. They also used the operative temperature as reference indoor temperature for total heat transfer determination. Through computational procedures, Kadarač [16] proposed general expressions for convective and overall coefficients considering air temperature as indoor reference temperature. ASHRAE also provides general expressions and charts to obtain cooling output estimations from ceiling surface temperature and indoor conditions [2].

However, most previous work is aimed at developing practical models to estimate the cooling output of particular types of radiant ceiling systems directly from the fluid supply temperature. This is the case of the theoretical investigation conducted by Antonopoulos et al. [17] as well as the simplified calculation method developed by Okamoto et al. [18]. Moreover, Jeong and Mumma [19, 20] developed a complete cooling capacity estimation method and evaluate the impact of various design parameters on the cooling output of the given system, including capacity enhancement under mixed convection conditions.

In any case, there are only a few published studies in order to establish the aforementioned general characteristic curve developed from ceiling surface temperature, and they even don't agree on its formal expression or the variables involved in these general correlations. Thus, the present study has the aim of providing further experimental evidence to better understand



heat transfer phenomena from radiant cooled ceiling surfaces and clarify ambiguous conceptions in cooling capacity estimations. To this end, an experimental facility for measuring system's cooling output is presented. Natural convection conditions and a sufficient wide range of temperatures are considered in the investigation. Heat transfer coefficients are also evaluated. Then, results are analyzed and compared with those found in literature. Finally, a preliminary discussion to derive a general trend which adequately explains data derived from different test conditions is presented.

3 Experimental setup

3.1 Climate test room

Tests were conducted in the climate test room shown in Figure 1, which is located inside a larger laboratory room with stable but not controlled temperature. It is characterized by a floor area of 12.96 m² (3.60 m x 3.60 m) and an internal height of 3.00 m. Floor is supported a small distance over the ground and is mainly composed by a 30 mm-thick chipboard and a PVC thin layer in the internal face. Walls are sandwich type, incorporating a 30 mm-thick extruded polystyrene (XPS) insulation between two layers made of sheet steel. Internal wall surfaces are characterized by an emissivity value of 0.8. Two sides of the test room façade show four windows (90 cm x 140 cm) and one glazed door (82 cm x 204 cm) in all, as can be observed in Figure 1. Double glazing with internal air chamber (4/6/4) is used. Test room ceiling is also insulated by a 4 mm fiberglass layer. Moreover, the test room is equipped with an air-to-air heat pump of an effective rated heating output of 2930 W. This machine includes an internal control which permits room air temperature to be fixed to an approximately constant value in each test. In order to avoid effects caused by high supply air velocity affecting convective phenomena inside the room, a small box with a lower opening was constructed in front of the supply section. In this way hot air slows down inside the box and enters the occupied zone with a very small velocity. In this way quite homogeneous air temperature conditions are achieved inside the test room and free convection is assured.

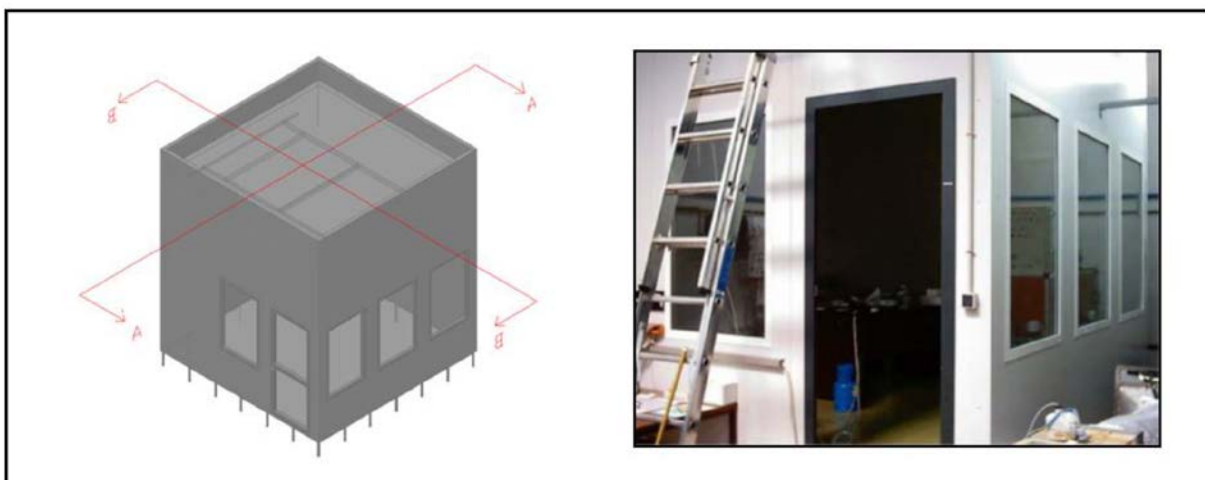


Fig. 1. General view of the climate test room (3.60 m × 3.60 m × 3.00 m).



3.2 Hydraulic circuit and ceiling panels

The hydraulic circuit is presented schematically in Figure 2. Two ceiling panels comprising corresponding pipe meshes made of polyethylene PE-RT 90 are arranged in a parallel assembly and fed directly from an unpressurized water tank. Each mesh is hydraulically balanced. Water is transported to the panels and returned to the tank through flexible 16mm-diameter reinforced polyurethane pipes. Also two T-shaped pipe fittings are placed at the inlet and outlet of the panels to make possible the aforementioned parallel assembly.

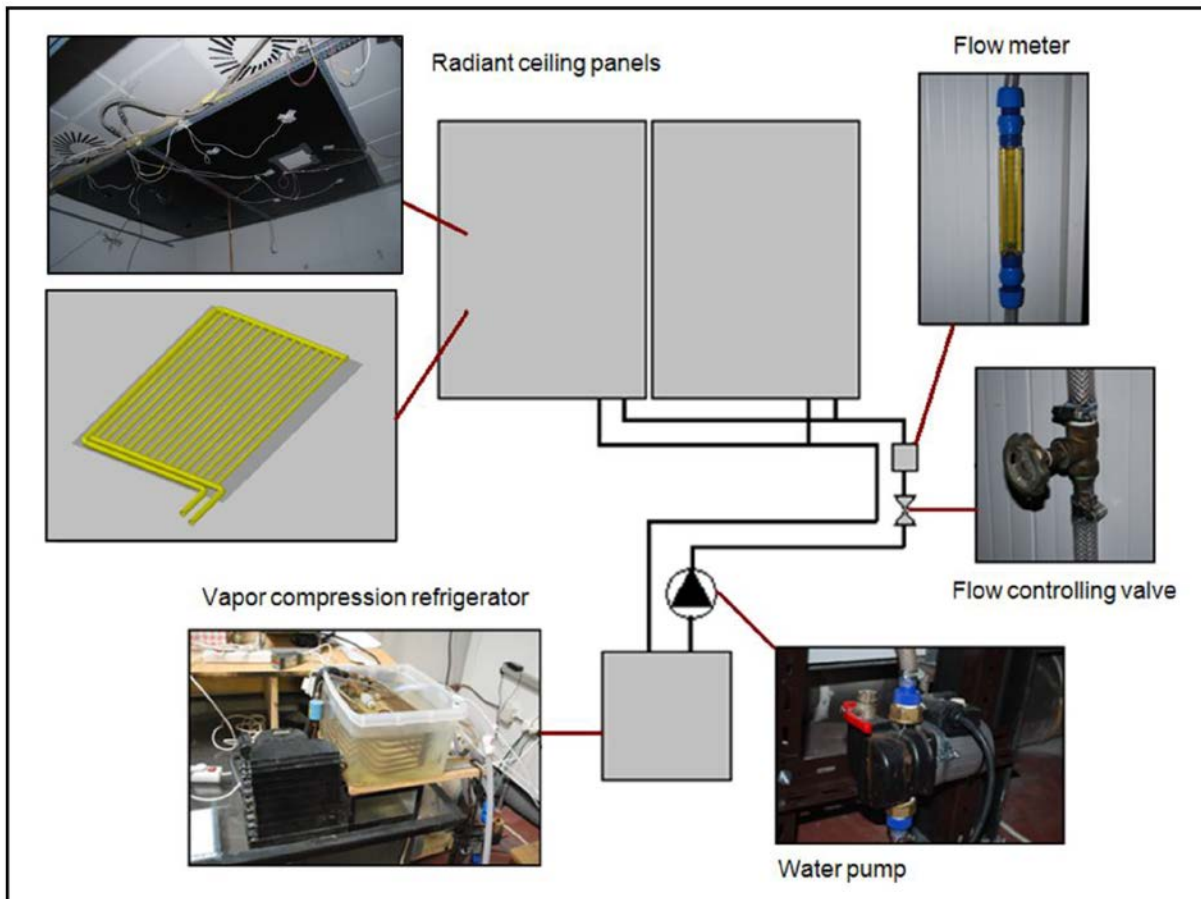


Fig. 2. Hydraulic circuit and installation components.

Figure 2 also presents a fluid pump with three different operation positions, a flow controlling valve and a flow meter which were mounted in the supply pipe. This set-up allows mass flow value to be fixed ranging from 2 to 7 kg/min.

Each of the two radiant panels installed inside the test room consists of a 1.26 m x 1.90 m aluminum sheet supported by a horizontal metallic structure placed at a height of 2.80 m. So, a total heat exchange area of 4.79 m² was available.

The water pipe mesh was stuck on the metal sheet using metallic adhesive tape over each single tube as it can be observed in Figure 3. Moreover, a 5cm-thick fiberglass layer was carefully laid over the pipes so that heat transfer from the cold water to the air in the upper zone was minimized and almost optimal heat conduction between pipes and metal sheet was assured. Originally, aluminum sheet surface facing downwards was characterized by a very



low emissivity value, so it reflected most of the heat radiation that it received. For this reason, an acrylic matt spray was used to paint this surface so that emissivity was increased to 0.8. This value was determined comparing measurements from a thermo-graphic camera and corresponding surface temperature sensors.

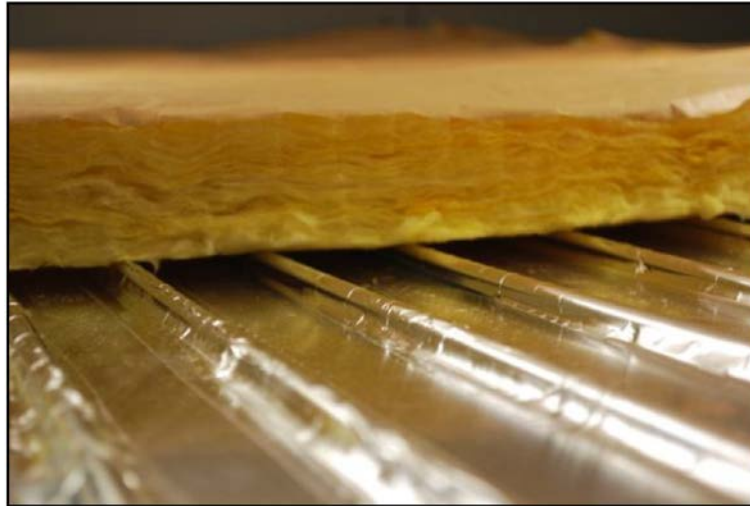


Fig. 3. Detailed view of the radiant panels.

3.3 Cold generation

Cold water is provided by a vapor compression refrigerator whose evaporator is immersed into the water tank, as shown in Figure 2. The refrigerator is operated through an on/off control according to an external signal allowing the supply temperature to be maintained approximately constant around a given setpoint. This on/off signal is generated by a simple controller connected to the compressor through a power contactor.

3.4 Measurement equipment

Measurements in the experimental facility were registered by means of different Pt100 temperature sensors (either ceramic-covered or thin-film type). Four-wire connections to the data acquisition equipment were employed. All the sensors were adequately calibrated in a temperature range between 0 °C and 40 °C. Calibration lines showed satisfactory linear behavior ($R^2 > 0.999$), which validates corrected measurements. A precision of ± 0.1 °C was provided.

A total number of 16 probes were used to measure wall, floor and cooled ceiling surface temperatures. They were conveniently coated with an insulation layer and stuck to the surface by a small piece of adhesive tape. Besides, four more temperature sensors with a radiant protection were placed in the vertical direction in the center of the room in order to observe air temperature stratification. Water temperature measurements were taken inside the water tank, and also at the inlet and outlet of the panel piping, where multiple probes were placed so as to increase accuracy. Outdoor air temperature was also registered by means of an extra sensor.



In addition, specific equipment was used to experimentally evaluate thermal comfort conditions in the center of the test room at an approximate 1.1 m height. This equipment includes three different probes, as shown in Figure 4:

- An omnidirectional anemometer measuring air velocity, turbulent intensity and air temperature.
- A specific operative temperature sensor, whose precise oval shape reproduces radiant heat exchange factors between human body and the surrounding surfaces.
- An air humidity sensor which also register air temperature.

From these measurements, data processing software provides values of different thermal comfort indexes derived from the Fanger's model, mainly Draught Risk (DR), Predicted Mean Vote (PMV) and Predicted Percentage Dissatisfied (PPD) [21]. 1.2 met and 0.8 clo were used as activity level and clothing insulation values.



Fig. 4. Thermal comfort measuring equipment.

4 Description of test conditions

The developed experimental program included 18 tests allowing for a range of operation conditions wide enough to the purpose of this research. Nine different combinations of indoor air temperature and water tank temperature setpoints were tested twice. 10, 14 and 17 °C water tank temperature setpoints were used, while internal control of the air-to-air heat pump was fixed at 23, 25 and 27 °C. Results are presented in Table 1 referencing each test by means of a two-number code according to these setpoints (for instance, 10/25 stands for 10 °C water temperature and 25°C air temperature). In this manner, various temperature differences between ceiling surface and room air were obtained.



Table 1. Main parameters determined for cooled radiant ceiling tests (Tests 1 – 18).

Test descriptor	1	2	3	4	5	6	7	8	9
	10/23	10/25	10/27	14/23	14/25	14/27	17/23	17/25	17/27
T_s (°C)	15.6	16.3	17.0	17.6	18.4	19.1	19.5	20.2	20.9
T_a (°C)	22.4	23.8	25.2	22,6	23.6	25.4	22,9	24.1	25.6
T_{op} (°C)	21.8	23.1	24.6	22,0	23.0	24.8	22.4	23.5	25.0
T_{mr} (°C)	21.2	22.5	24.0	21,4	22.4	24.1	21.8	22.9	24.3
AUST (°C)	20.5	21.5	23.1	20,6	21.5	23.0	21.1	22.0	23.4
q_r (Wm^{-2})	25.7	27.9	32.9	16,7	16.7	21.6	9.0	10.1	13.8
h_r ($Wm^{-2}K^{-1}$)	5.3	5.3	5.4	5,5	5.4	5.5	5.4	5.5	5.5
q_c (Wm^{-2})	29.1	26.5	38.0	17,8	26.1	26.6	14.6	17.1	18.9
h_c ($Wm^{-2}K^{-1}$)	4.3	3.5	4.6	3,6	5.0	4.2	4.2	4.3	4.0
q_{tot} (Wm^{-2})	54.7	54.4	70.9	34,5	42.8	48.1	23.6	27.2	32.7
h_{tot} ($Wm^{-2}K^{-1}$)	8.8	7.9	9.3	7,8	9.3	8.5	8.2	8.1	8.1
Test descriptor	10	11	12	13	14	15	16	17	18
	10/23	10/25	10/27	14/23	14/25	14/27	17/23	17/25	17/27
T_s (°C)	15.6	16.3	17.4	17.8	18.4	19.8	19.4	20.5	21.2
T_a (°C)	22.7	24.1	25.7	22.6	24.0	26.3	22.5	24.8	26.2
T_{op} (°C)	22.1	23.5	25.1	22.0	23.4	25.7	21.9	24.2	25.5
T_{mr} (°C)	21.5	22.9	24.5	21.4	22.8	25.0	21.3	23.6	24.9
AUST (°C)	20.8	22.4	23.4	20.6	22.1	24.2	20.5	23.0	23.7
q_r (Wm^{-2})	27.8	32.4	32.6	15.2	19.9	24.3	5.9	13.7	14.0
h_r ($Wm^{-2}K^{-1}$)	5.3	5.3	5.4	5.3	5.4	5.5	5.4	5.5	5.5
q_c (Wm^{-2})	29.5	27.6	36.0	18.0	22.2	28.0	17.0	15.7	22.8
h_c ($Wm^{-2}K^{-1}$)	4.2	3.5	4.4	3.7	3.9	4.3	5.6	3.7	4.6
q_{tot} (Wm^{-2})	57.3	60.0	68.6	33.2	42.1	52.3	22.9	29.3	36.8
h_{tot} ($Wm^{-2}K^{-1}$)	8.8	8.3	8.9	7.8	8.4	8.9	9.3	8.0	8.5

Besides, test conditions guaranteed a good quality of the indoor thermal environment. Indeed, thermal comfort levels were measured and proved to be maintained within an appropriate range (PPD<10%) during all the experiments, according to standards normally accepted [22]. Moreover, a water mass flow value of 3 kg/min, that is to say 0.626 kg/(min·m²), was supplied in every test. Nevertheless, some extra checking tests were conducted previously in order to prove that different mass flow values did not highly affect cooling output results. This could be justified because convection-radiation thermal resistance between ceiling surface and its surroundings dominates over conduction resistance between water and ceiling surface. Lower mass flows were not chosen as slight mismatch between pressure drops in different panel circuits did not allow homogeneous flow distribution to be achieved. On the other hand, higher mass flows would have implied loss of accuracy in heat flux measurements due to smaller water temperature differences between panel inlet and outlet.



Average test duration was set around 4 hours so that all interesting variables reached a steady state situation. Nevertheless, results presented in Table 1 correspond to average values calculated during periods of at least 30 minutes in which stable conditions were observed.

5 Determination of main parameters

Determination of measured and calculated parameters which are shown in Table 1 is commented next:

T_a values correspond to those registered by the thermal comfort measuring equipment at an approximate height of 1.1 m in the center of the test room. It can be observed that these values are not the same as corresponding fixed setpoints, which indicates that heat pump internal control is not ideal. However, control is good enough for the purpose of this research as indoor air temperature values are clearly distinct for each different control setpoint.

The operative temperature (T_{op}) is also experimentally determined by the thermal comfort measuring equipment. T_{op} is defined as the weighted average value between the air dry-bulb temperature and the mean radiant temperature. According to ASHRAE Standard 55 [23], when very low air velocity values are registered, these weights are both equal to 0.5. This hypothesis can be assumable for the developed test conditions here, so T_{mr} is calculated according to expression Eq. (2) from operative temperature (T_{op}) and T_a values, without incurring in relevant error.

$$T_{op} \approx T_{ad} = \frac{T_a + T_{mr}}{2} \rightarrow T_{mr} \approx 2T_{op} - T_a \quad (2)$$

AUST represents the weighted average temperature of a fictitious surface considering all surfaces other than the panel. Thus, it could be defined as an area-weighted average temperature [2]. Nevertheless, determination based on view factors is more precise [15]. Expression Eq. (3) shows the exact definition used in this work.

$$AUST = \sqrt[4]{\sum_j F_{s-j} \cdot (273.15 + T_j)^4} \quad (3)$$

Floor and wall surface temperature values were taken from experimental measurements. In addition, homogeneous temperature distribution was assumed for each surface. View factors were calculated through numerical evaluation of the corresponding integral expressions [24]. Results of such calculations are shown in Table 2.

Cooling capacity, expressed in terms of heat flux density through the ceiling surface, is obtained directly from experimental measurements of water mass flow and water temperature difference between the inlet and the outlet of the panels, as stated in Eq. (4).

$$q_{tot} = \frac{1}{A_s} [m_w c_{p,w} (T_{w,in} - T_{w,out})] \quad (4)$$

Table 2. View factors considered for AUST determination.



Surfaces	View factors (F_{s-j})
Wall 1	$F_{s-1} = 0.1770$
Wall 2	$F_{s-2} = 0.1643$
Wall 3	$F_{s-3} = 0.1770$
Wall 4	$F_{s-4} = 0.1643$
Floor	$F_{s-5} = 0.3174$

Thermal insulation placed over the water pipes in the panels allows neglecting heat gains other than those due to the heat transfer through the aluminum sheet lower surface.

Determination of radiant heat flux density to the panels has been developed according to a standard procedure based on theoretical considerations on radiant heat transfer between grey surfaces [2, 15, 24, 25]. Thus, q_r is expressed as:

$$q_r = \frac{\sigma}{A_s} \left[\sum_j F_{\varepsilon_{s-j}} \cdot [(273.15 + T_j)^4 - (273.15 + T_s)^4] \right] \quad (5)$$

where $F_{\varepsilon_{s-j}}$, according to Eq. (6), takes into account emissivity values of every surface involved.

$$F_{\varepsilon_{s-j}} = 1 / \left[\left(\frac{1 - \varepsilon_s}{\varepsilon_s} \right) + \left(\frac{1}{F_{s-j}} \right) + \left(\frac{A_s}{A_j} \right) \left(\frac{1 - \varepsilon_j}{\varepsilon_j} \right) \right] \quad (6)$$

Cooled ceiling surface emissivity value of 0.8 was used in calculations. On the other hand, 0.9 was considered for the other surfaces. Both values were obtained experimentally from surface temperature measurements and corresponding thermographic images.

Convective heat flux density was determined as the difference between total and radiant values.

Furthermore, heat transfer coefficients (convective, radiant and total) were calculated through the same formal expression (Eq. (7)) conveniently applied in each particular case.

$$h = q / (T_{ref} - T_s) \quad (7)$$

In this expression, T_{ref} represents a given reference temperature whose definition in each case is not clearly agreed by different authors. Results presented in this study were obtained in accordance with the proposal of Causone et al. [15], as it was considered acceptable a priori. In this manner, data for comparison is provided as well. Thus, $AUST$, T_a and T_{op} were respectively used as reference temperatures in radiant, convective and total heat transfer coefficient calculations.

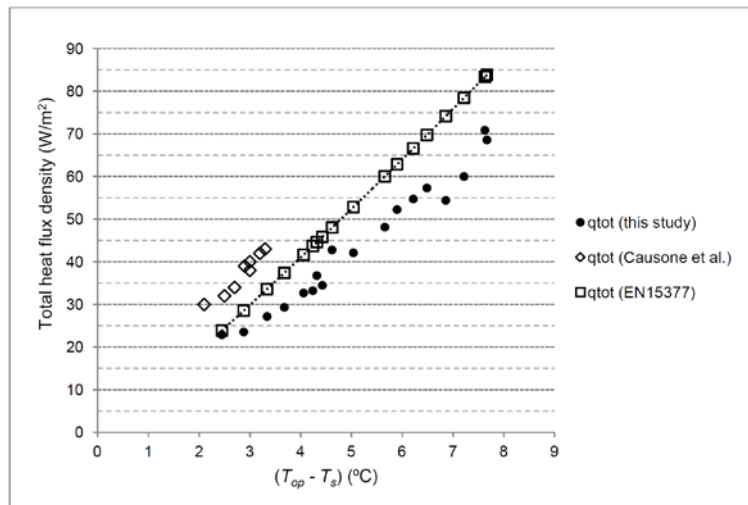


Fig. 5. Total cooling capacity for a radiant cooled ceiling.

6 Results and discussion

Numerical results derived from the 18 radiant ceiling cooling tests are presented in Table 1, and discussed next:

6.1 Cooling output

Figure 5 shows total cooling capacity as a function of temperature difference ($T_{op}-T_s$). Data derived from tests in this research and also those from literature [14, 15] are presented. Cooling output increases with growing temperature differences as expected. Nevertheless, each group of data follows a different trend line. Particularly, in this work, lower total heat flux densities for each ($T_{op}-T_s$) value were obtained.

An explanation to these differences could be provided considering radiant and convective heat transfer separately. Figure 6 and Figure 7 show radiant and convective heat flux densities as a function of the difference between correspondent reference temperature (AUST or T_a) and ceiling surface temperature. Tests developed in this study were compared to those from Causone et al. [15]. Values from the standard EN 15377-1 [14] were not analyzed because specific experimental information is not available. Moreover, it should be mentioned that convective heat flux density values show higher dispersion than that of the radiant ones. This may happen because radiant heat transfer was determined based on a theoretical model, so experimental error in total heat transfer measurements was completely assigned to convective values.

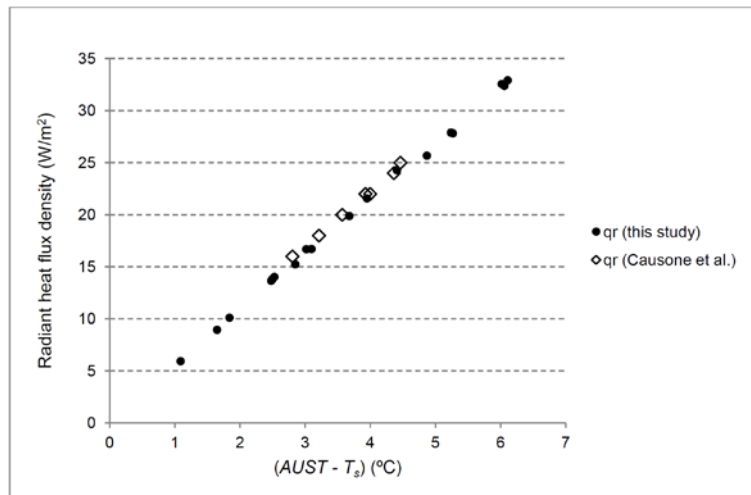


Fig. 6. Radiant heat flux density.

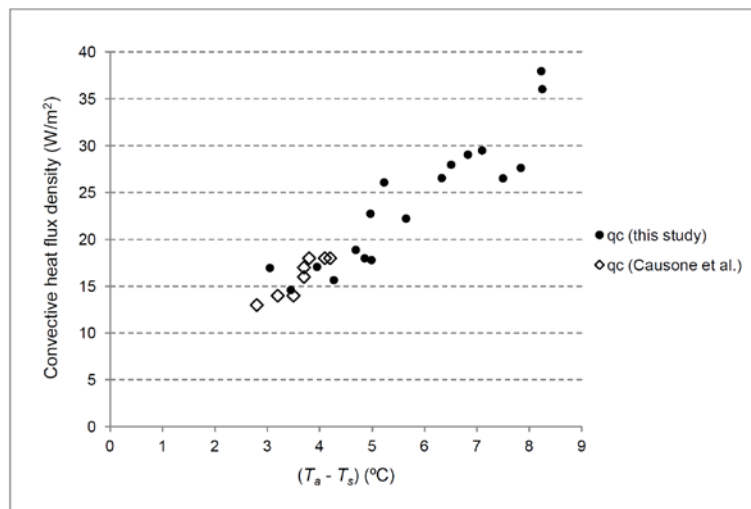


Fig. 7. Convective heat flux density.

Anyway, it can be noticed that groups of values from both studies show same behavior patterns. Indeed, same heat flux density values were obtained for comparable temperature differences.

However, the reason why same total heat dissipation rate dependences on $(T_{op}-T_s)$ were not observed in different studies is that the same operative temperature can be derived from multiple different combinations of AUST and T_a , depending mainly on particular characteristics of insulation and outdoor environment, and thus causing quite distinct q_{tot} . Thus, total cooling capacity of the radiant ceiling cannot be determined attending to the operative temperature (T_{op}) as the only reference temperature, but taking into consideration both radiant and convective heat fluxes and respective reference temperatures in a separate way.

6.2 Heat transfer coefficients

Radiant, convective and total heat transfer coefficient values for a cooled radiant ceiling system determined in this research are included numerically in Table 1 and also graphically presented in Figure 8. A comparison with previous data found in literature is shown in Table 3 as well.



Radiant heat transfer coefficient can be considered constant ($5.4 \text{ Wm}^{-2}\text{K}^{-1}$). This fact is conveniently justified in literature [15] and confirms data obtained in those studies. Nevertheless, slightly lower values shown here can be explained by the influence of the ceiling surface emissivity ($\epsilon_s=0.8$), which is a bit smaller than values associated to common construction materials.

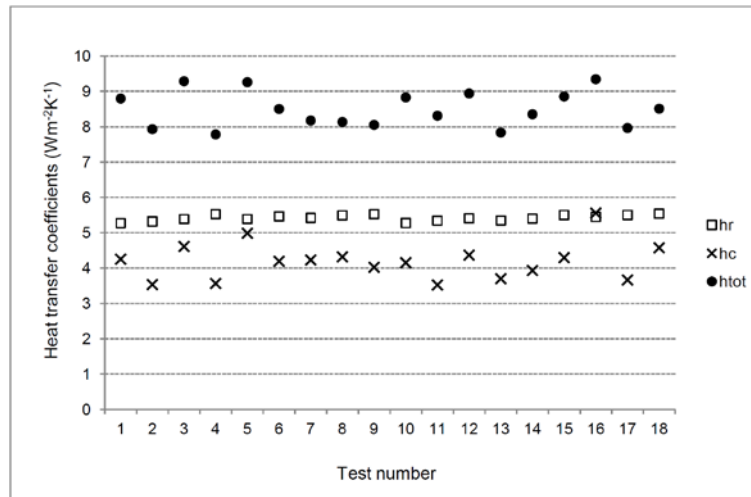


Fig. 8. Heat transfer coefficients for a radiant cooled ceiling (present study).

An average convective heat transfer coefficient of $4.2 \text{ Wm}^{-2}\text{K}^{-1}$ was derived from the present work. This value is consistent with those found in literature for a heated floor or a cooled ceiling configuration, which are between 2.8 and $4.8 \text{ Wm}^{-2}\text{K}^{-1}$ when temperature difference moves from $3 \text{ }^\circ\text{C}$ to $9 \text{ }^\circ\text{C}$, as in the tests conducted here.

Table 3. Comparison between heat transfer coefficients determined in this work and reference literature values.

Source	h_c ($\text{Wm}^{-2}\text{K}^{-1}$)	h_r ($\text{Wm}^{-2}\text{K}^{-1}$)	h_{tot} ($\text{Wm}^{-2}\text{K}^{-1}$)
Causone et al. [15] ^a	4.4	5.6	13.2
EN 15377-1 [14]	-	-	10 – 11.1
ASHRAE [2]	3.1 – 4.3	-	-
Khalifa et al. [26]	3.1 – 3.6	-	-
Min et al. [27]	3.6 – 4.8	-	-
Awbi et al. [28]	2.8 – 3.9	-	-
Present study ^a	4.2	5.4	8.5

^a Average values derived from corresponding experimental research.

Furthermore, total heat transfer coefficients range from 7.8 to $9.3 \text{ Wm}^{-2}\text{K}^{-1}$ resulting in an average value of $8.5 \text{ Wm}^{-2}\text{K}^{-1}$. Contrary to what happens with radiant and convective heat transfer coefficients, which are consistent to those reported in previous works, total coefficient is clearly lower than those from literature ($10 - 13.2 \text{ Wm}^{-2}\text{K}^{-1}$) [10, 14, 15, 25].

As exposed in section 6.1, these differences can be explained by different test conditions regarding combinations of AUST and T_a for a given T_{op} value. According to this argumentation, the calculation of total heat transfer coefficient only based on the operative temperature as



reference, neither provides full knowledge of the heat transfer process nor is appropriate to estimate cooling output of the radiant cooled ceiling system. It would only be representative in specific situations when $AUST$, T_a and T_{op} values approximately coincide, like in rooms with really high wall insulation. However, real situations are mostly characterized by differences between internal surface temperatures and room air temperature. This is the reason why this parameter should not be used for design purposes, but radiant and convective heat transfer coefficients should be calculated and applied separately.

7 Conclusion

In this work, an experimental facility was developed in order to characterize a radiant cooled ceiling allocated in a climate test room. Results obtained proved that this setup is suitable to determine system's cooling output and validated it for future work on energy use and thermal comfort issues regarding radiant ceiling cooling.

Further experimental evidence on the cooling capacity and heat transfer coefficients for a cooled ceiling system was provided. Approximate average values of $5.4 \text{ Wm}^{-2}\text{K}^{-1}$ and $4.2 \text{ Wm}^{-2}\text{K}^{-1}$ were respectively found for radiant and convective heat transfer coefficients. Both are consistent with data previously reported in other works. However, an average total heat transfer coefficient of $8.5 \text{ Wm}^{-2}\text{K}^{-1}$ was obtained, which is quite lower than those from literature.

Total cooling capacity for different $(T_{op}-T_s)$ did not follow expected behavior patterns according to previous research, but it showed quite lower values. Nevertheless, separate analysis of radiation and convection heat fluxes revealed that data from different studies actually adequate to the same trends.

Consequently, regarding design purposes in real situations, it is argued that cooling output of a radiant cooled ceiling can neither be studied nor predicted on the basis of the operative temperature as the unique reference temperature and its corresponding coefficient. Thus, considering both radiant and convective phenomena separately is needed.

Nomenclature

A:	area (m^2)
AUST:	average unheated (uncooled) surface temperature ($^{\circ}\text{C}$)
C_p :	specific heat capacity ($\text{J kg}^{-1} \text{K}^{-1}$)
F_{es-j} :	radiation interchange factor
F_{s-j} :	view factor between cooled radiant surface and j-surface
h:	heat transfer coefficient ($\text{W m}^{-2} \text{K}^{-1}$)
m:	Mass flow (kg/s)
q:	heat flux density (W m^{-2})
T_a :	indoor air dry bulb temperature ($^{\circ}\text{C}$)
T_{mr} :	mean radiant temperature ($^{\circ}\text{C}$)
T_{op} :	operative temperature ($^{\circ}\text{C}$)
T_s :	cooled radiant ceiling surface temperature ($^{\circ}\text{C}$)
T_w :	water temperature ($^{\circ}\text{C}$)
ϵ :	emissivity
σ :	Stefan-Boltzmann constant ($\text{Wm}^{-2}\text{K}^{-4}$)



Subscript

a:	air
c:	convective
j:	j-surface
r:	radiant
s:	cooled ceiling surface
tot:	total
w:	water
in:	ceiling panel inlet
out:	ceiling panel outlet

Acknowledgements

Manuel Andrés-Chicote wishes to thank the Spanish Government for the support given through a FPU (Formación de Profesorado Universitario) scholarship. Reference: AP2010-2449.

References

- [1] EPBD recast: Directive 2010/31/EU of the European Parliament and of the Council of 19 May 2010 on the Energy Performance of Buildings (recast). <http://eur-lex.europa.eu/LexUriServ/LexUriServ.do?uri=OJ:L:2010:153:0013:0035:EN:PDF>
- [2] ASHRAE Systems and Equipment Handbook. Chapter 6: Panel Heating and Cooling.
- [3] J. Miriel, L. Serres, A. Trombe, Radiant ceiling panel heating-cooling systems: experimental and simulated study of the performances, thermal comfort and energy consumptions. *Applied Thermal Engineering* 22 (2002) 1861-1873.
- [4] Mostafa Rahimi, Amir Sabernaemi, Experimental study of radiation and free convection in an enclosure with a radiant ceiling heating system, *Energy and Buildings* 42 (2010) 2077-2082.
- [5] F.P. Incropera, D.P. DeWitt, *Fundamentos de Transferencia de Calor*, 4a ed, Pearson, Prentice-Hall, 1999.
- [6] D. Saelens, W. Parys, R. Baetens, Energy and comfort performance of thermally activated building systems including occupant behavior, *Building and Environment* 46 (2011) 835-848.
- [7] F.J. Rey Martínez, E. Velasco Gómez, A. Tejero González, F.E. Flores Murrieta, Comparative study between a ceramic evaporative cooler (CEC) and an air-source heat pump applied to a dwelling in Spain, *Energy and Buildings* 42 (2010) 1815-1822
- [8] B. Costelloe, D. Finn, Indirect evaporative cooling potential in air-water systems in temperate climates, *Energy and Buildings* 35 (2003) 573-591.
- [9] Xinhua Xu, Shengwei Wang, Jinbo Wang, Fu Xiao, Active pipe-embedded structures in buildings for utilizing low-grade energy sources: A review, *Energy and Buildings* 42 (2010) 1567-1581.
- [10] J. Babiak, B.W. Olesen, D. Petráš, Low temperature heating and high temperature cooling, *Guidebook NO 7*, REHVA, 2009.



- [11] B. Lehmann, V. Dorer, M. Koschenz, Application range of thermally activated building systems tabs, *Energy and Buildings*, 39 (2007) 593-598.
- [12] B. Lehmann, V. Dorer, M. Gwerder, F. Renggli, J. Tödtli, Thermally activated building systems (TABS): Energy efficiency as a function of control strategy, hydronic circuit topology and (cold) generation system, *Applied Energy* 88 (2011) 180-191.
- [13] D.O. Rijksen, C.J. Wisse, A.W.M. van Schijndel, Reducing peak requirements for cooling by using thermally activated building systems, *Energy and Buildings* 42 (2010) 298-304.
- [14] Design of embedded water based surface heating and cooling systems - Part 1: determination of the design heating and cooling capacity. Standard EN 15733-1. Comité Européen de Normalisation; 2005.
- [15] Causone, F., Corgnati, S.P., Filippi, M., Olesen, B.W. Experimental evaluation of heat transfer coefficients between radiant ceiling and room. *Energy and Buildings* 41 (2009) 622-628.
- [16] Refet Kadarađ, New approach relevant to total heat transfer coefficient including the effect of radiation and convection at the ceiling in a cooled ceiling room, *Applied Thermal Engineering* 29 (2009) 1561-1565.
- [17] K. A. Antonopoulos, M. Vrachopoulos, C. Tzivanidis, Experimental and theoretical studies of space cooling using ceiling-embedded piping. *Applied Thermal Engineering* 17 (1997) 351-367.
- [18] Shigeru Okamoto, Hisataka Kitora, Hiromasa Yamaguchi, Tatsuo Oka, A simplified calculation method for estimating heat flux from ceiling radiant panels. *Energy and Buildings* 42 (2010) 29-33.
- [19] Jae-Wong Jeong, Stanley A. Mumma, Ceiling radiant cooling panel capacity enhanced by mixed convection in mechanically ventilated spaces. *Applied Thermal Engineering* 23 (2003) 2293-2306.
- [20] Jae-Wong Jeong, Stanley A. Mumma, Practical cooling capacity estimation model for a suspended metal ceiling radiant cooling panel. *Building and Environment* 42 (2007) 3176-3185.
- [21] Fanger, P.O. *Thermal Comfort*. McGraw-Hill, (1972).
- [22] Ergonomics of the thermal environment – Analytical determination and interpretation of thermal comfort using calculation of the PMV and PPD indices and local thermal comfort criteria. Standard EN ISO 7730. Brussels. Comité Européen de Normalisation; 2005.
- [23] ASHRAE Standard 55:2004, *Thermal Environmental Conditions for Human Occupancy*.
- [24] F. Kreith, M.S. Bohn, *Principios de Transferencia de Calor*. 6ª ed. Thomson, 2002.
- [25] F.J. Rey Martínez, E. Velasco Gómez, DTIE 9.04. *Sistema de suelo radiante*. ATECYR, 2008.



- [26] Khalifa, A.J.N., Marshall, R.H., Validation of heat transfer coefficients on interior building surfaces using real-sized indoor test cell. *International Journal of Heat and Mass Transfer* 33 (1990) 2219-2236.
- [27] Min, T.C., Schutrum, L.F., Parmelee, G.V., Vouris, J.D. Natural convection and radiation in a panel-heated room. *ASHRAE Trans*, 62 (1956), 337-58.
- [28] Awbi, H.B., Hatton. A., Natural convection from heated room surfaces. *Energy and Buildings* 30 (1999) 233-244.